Optimal power-splitting strategy via MPC for fuel cell hybrid electric vehicles

Roberto Rocco*, William Notaro†, Chiara Panagrosso‡
Università degli Studi di Napoli Federico II, Napoli
Email: *roberto.rocco3, †w.notaro, ‡c.panagrosso@studenti.unina.it

***Abstract*—Fuel cell electric vehicles (FCEVs) are often considered a promising solution for sustainable transportation, but their high ownership costs hinder competitiveness in today's auto market. To enhance the economic viability of fuel cell/battery-based hybrid electric vehicles, this paper introduces a real-time cost-minimization energy management strategy aimed at reducing operating costs. This strategy employs model predictive control, integrating both hydrogen consumption and energy source degradation into a multi-objective cost function. Utilizing forecasted speed data, dynamic programming is used to determine the optimal power-splitting decisions over each receding horizon. The strategy's performance is evaluated by examining the impact of various factors, such as battery state-of-charge regulation coefficients and prediction horizon lengths. A comparative study demonstrates the strategy's effectiveness, showing an average reduction in operating costs by 14.17% and an 8.48% increase in fuel cell lifespan compared to a rule-based benchmark.**

1. Introduction

As fuel cell technologies continue to advance, fuel cell hybrid electric vehicles (FCHEVs) are increasingly recognized as a promising alternative to traditional internal combustion engine (ICE) hybrid electric vehicles (HEVs). However, the high total ownership costs of FCHEVs, particularly the significant expenses associated with onboard fuel cell and battery systems, present a barrier to widespread adoption. A major contributor to these costs is hydrogen consumption, exacerbated by the limited availability of hydrogen refueling stations and the high price of green hydrogen. Additionally, the cost is impacted by the susceptibility to damage of some components, such as proton exchange membrane fuel cells (PEMFCs) and batteries, from improper usage, which can shorten their lifespan and increase maintenance costs.

To address these challenges, optimizing the use of the hybrid powertrain is crucial for reducing operating costs. This optimization is often achieved through effective energy management strategies (EMS), which coordinate the outputs of multiple energy sources to meet power demands while maximizing economic benefits.

Optimization-based strategies, formulate energy management tasks as mathematical optimization problems, which can be addressed by techniques such as dynamic programming (DP). For example, DP has been employed to minimize hydrogen consumption or operating costs, considering factors such as battery SoC deviations and hydrogen costs. Despite their effectiveness, DP can be computationally intensive.

In the realm of control techniques, model predictive control (MPC) is prominent. It anticipates future power needs based on a finite time horizon and makes control decisions accordingly. The effectiveness of MPC is highly dependent on the accuracy of predictions for future disturbances.

Some existing optimization-based EMSs focus solely on minimizing hydrogen consumption, neglecting the impact of energy source degradation on operating costs. Multi-objective EMSs have emerged to address these limitations by integrating factors like fuel cell efficiency and degradation into the optimization process. These approaches aim to balance hydrogen consumption with the health of the fuel cell and battery systems.

To address these gaps, this paper proposes a cost-minimization strategy using MPC for FCHEVs. The objectives of this work include:

1) **Development of a predictive control strategy:** This strategy reduces operating costs by considering both hydrogen consumption and energy source degradation. We assume to have perfect information on future disturbances (vehicle speed).
2) **Sensitivity analysis:** The impact of some factors, including SoC weighting coefficients, and prediction horizon length, on EMS performance is examined.
3) **Comparative evaluation:** The proposed strategy is tested against three benchmark approaches under various driving conditions to demonstrate its effectiveness in reducing operating costs and extending fuel cell lifespan.

2. System Modelling

This section presents the modelling of the studied fuel cell electric vehicle, including the vehicle's structure, the powertrain topology, and the models of fuel cell, battery and electric machine.

2.1. Vehicle structure and powertrain topology

As displayed in Fig. 2(a), this paper concentrates on a midsize sedan model, extracted from the vehicular simulator ADVISOR [1] and modified to introduce a fuel cell system as primary source. Fig. 2(b) schemes the studied hybrid propulsion system, which comprises a PEMFC system and a battery pack. A unidirectional DC-DC converter is attached to the PEMFC

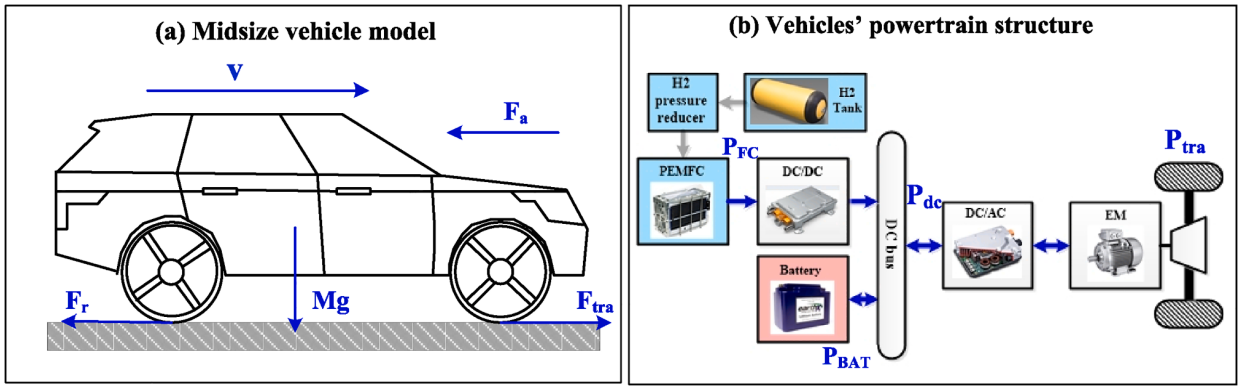

Figure 1. Studied vehicle model: (a) midsize vehicle outline and (b) topology of the hybrid powertrain.

output end, with the purpose of regulating fuel cell current towards the DC bus, while the battery is straight plugged to the DC bus. Since the battery is not equipped with the plug-in property, it can only be recharged via DC bus by PEMFC or by the regenerative energy. The sizes and main vehicular specifications are listed in the referenced Author's article [2].

When the propulsion power (P_{tra}) requested by the driving cycle is specified, the output power from PEMFC (P_{FC}) and battery (P_{BAT}) jointly response to the DC bus power demand (P_{DC}). Specifically, such power balance relationship can be expressed by Eqs. (1) and (2).

$$P_{tra} = v \cdot F_{tra} = v \cdot \left[c_r M g \cos(\vartheta) + 0.5 \rho_{air} S_f c_d v^2 + M\dot{v} \right] \quad (1)$$

$$P_{dc} = \frac{P_{tra}}{\eta_{drive} \cdot \eta_{DC/AC} \cdot \eta_{EM}} = P_{BAT} + P_{FC} \cdot \eta_{DC/DC} \quad (2)$$

where v is vehicle speed, c_r the coefficient of rolling resistance, M the vehicle weight, g the gravitational acceleration, ρ_{air} the density of ambient air, S_f the area of vehicle front surface, c_d the coefficient of aerodynamic drag, η_{drive}, $\eta_{DC/AC}$, $\eta_{DC/DC}$ and η_{EM} the efficiency of drive line, DC-AC inverter, DC-DC converter and electric machine, respectively. Moreover, the road slope ϑ is assumed to be zero.

2.2. *Fuel Cell Model*

PEMFC is the primary energy source in the hybrid powertrain. This study adopts a 300-cell PEMFC system with the rated (net) power at 30 kW. As the core of PEMFC system, fuel cell stack converts hydrogen energy into useful electrical power (P_{stack}) via a series of electrochemical reactions. A fraction of electrical power (P_{AUX}) generated by the stack is used in auxiliary devices (e.g. air compressor, etc.) while the actual output (net) power from PEMFC system (P_{FC}) equals to the difference between P_{stack} and P_{AUX}. During the operation of PEMFC, the hydrogen mass consumption (M_{H_2}) can be calculated by:

$$M_{H_2} = \int_0^t \frac{P_{FC}}{\eta_{FCS} \cdot LHV_{H_2}} d\tau \quad (3)$$

Where $\eta_{FCS} = P_{FC}/P_{H_2}$ is the efficiency of PEMFC system, P_{H_2} the theoretical power supplied by H2 and LHV_{H_2} the H2 lower heating value (120,000 J/g). To calculate the H2 mass consumption, it is necessary to quantify the relationship between P_{FC} and P_{H_2}. As shown in Fig. 2(b), the efficiency curve (blue solid line) of the studied 30-kW PEMFC system is obtained from the scaled version of the FC_ANL50H2 model in ADVISOR, where the red dashed curve depicts the relationship between P_{FC} and P_{H_2}. To facilitate the calculation of H2 consumption, a quadratic fitted H2 power model is given as (4), where $a_0 = 2.39312$, $a_1 = 1.15$, $a_2 = 0.0238$ are the fitting coefficients.

$$P_{H_2} = a_2 \cdot P_{FC}^2 + a_1 \cdot P_{FC} + a_0 \quad (4)$$

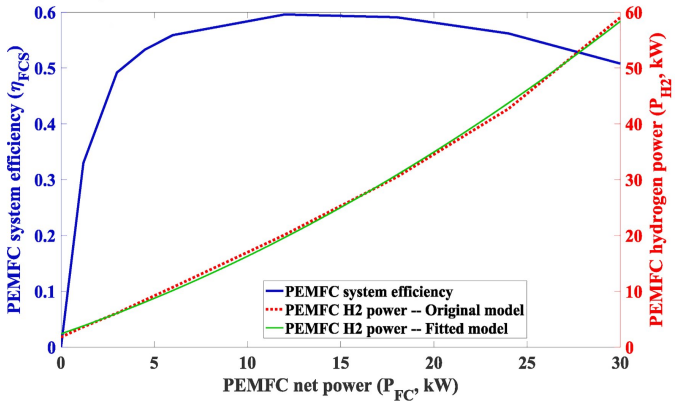

Figure 2. PEMFC system efficiency and estimated H2 power as a function of P_{FC}

Besides, modelling the degradation of PEMFCs requires an in-depth understanding on the fuel cell degrading mechanism, which is a complex process involving multiple impact factors. To sum up, four PEMFC operating conditions, namely start-stop cycling, transient loading, high and low loading, are the primary factors causing its performance degradation. In this study, the cell voltage drop rate per on-off cycle α_{on-off} is adopted to describe such degrading effect. As for other degrading effects, the PEMFC high loadings are defined as when $P_{FC} \geq 0.8 \cdot P_{FC}^{max}$, and the PEMFC low loadings are defined as when $P_{FC} \leq 0.2 \cdot P_{FC}^{max}$, where $P_{FC}^{max} = 30$kW is the rated power of PEMFC.

α_{high} and α_{low} respectively denote the cell voltage degradation rate per hour at high and low loadings. In addition, when fuel cell transient load appears, the cell voltage degrading rate is described by α_{shift}. Besides, it is assumed that the mentioned degrading factors are independent of each other, and, thereby, their degrading effects can be simply added up to calculate the entire voltage degradation (in μV).

2.3. Battery model

This paper adopts a 970-cell lithium-ion battery pack as the secondary energy source in the hybrid powertrain, with its nominal energy capacity being 7.4 kWh (320 V/23Ah). The feature of a single battery cell is extracted from the published datasheet of A123 Systems ANR26650M1 cell (3.3 V/2.3Ah). It is assumed an R-int model for the battery pack. Given the open-circuit voltage (U_{OC}) and the internal resistance (R_{BAT}) of battery pack, according to Kirchhoff's voltage law, the DC bus voltage (U_{dc}) can be expressed as:

$$U_{DC} = U_{OC} - I_{BAT} \cdot R_{BAT} \tag{5}$$

Combine (5) with the expression of battery output power $P_{BAT} = U_{dc} \cdot I_{BAT}$, battery current I_{BAT} can thus be calculated by:

$$I_{BAT} = \frac{U_{OC}(SoC) - \sqrt{U_{OC}(SoC)^2 - 4 \cdot R_{BAT}(SoC) \cdot P_{BAT}}}{2 \cdot R_{BAT}(SoC)} \tag{6}$$

where U_{OC} and R_{BAT} can be expressed as functions of battery SoC.

Such feature is available in the datasheet of the studied battery cell. In addition, SoC is a percentage indicator of the remaining battery capacity (in Ah) versus its nominal one, with its dynamics given as:

$$SoC(t) = SoC_{ini} - \int_0^t \frac{\eta_{BAT} \cdot I_{BAT}(\tau)}{Q_{BAT}} d\tau \tag{7}$$

where Q_{BAT} is the nominal capacity of battery pack (Ah), SoC_{ini} the initial SoC, and η_{BAT} the battery efficiency.

With the usage of battery in delivering or recovering electrical power, its performance gradually degrades owing to the irreversible physical and electrochemical changes. One of the significant phenomena during battery aging is the fade of capacity. To estimate the battery capacity loss, a control-oriented battery degrading model is adopted in this work (see Authors' reference [37]). According to the Arrhenius equation, the percentage loss of battery cell capacity ΔQ_{cell} (%) with respect to its initial capacity (100%) can be expressed by:

$$\Delta Q_{cell} = B(c_{rate}) \cdot \exp\left(\frac{-E_a(c_{rate})}{RT}\right) (A_h(c_{rate}))^z \tag{8}$$

where c_{rate} is the battery current c-rate, B is the pre-exponential coefficient, which is a function of c_{rate}. This parameter can be found in Authors' article. Moreover, Ea is the activation energy, R the constant of ideal gas (8.31 J/mol), T the battery cell temperature (assumed as 298.2 K (25 °C)), the Ah-throughput A_h is the amount of electric charge delivered by battery during cycles, and z is the power-law coefficient. Based on the experimental-fitted data from the article, z takes 0.55 and the expression of E_a is denoted by:

$$E_a = 31700 - 370.3 \cdot c_{rate} (J/mol \cdot K) \tag{9}$$

A 20% capacity fade is normally deemed as the end-of-life (EoL) of a power battery, and thus the corresponding Ah-throughput (A_h^{EoL}) can be derived by solving (10):

$$A_h^{EoL}(c_{rate}) = \left[\frac{20}{B(c_{rate}) \cdot \exp\left(\frac{-E_a(c_{rate})}{RT}\right)}\right]^{1/z} \tag{10}$$

Hence, the total number of cycles (NEoL) until the battery EoL can be obtained by:

$$N_{EoL}(c_{rate}) = \frac{A_h^{EoL}(c_{rate})}{Q_{cell}} \tag{11}$$

On this basis, the battery state-of-health ($SoH(t) \in [0, 1]$) is defined as follows:

$$SoH(t) = 1 - \frac{\int_0^t |i_{cell}(\tau)| \, d\tau}{2 \cdot N_{EoL}(c_{rate}) \cdot Q_{cell}} \tag{12}$$

where the initial SoH is assumed to be 100% and i_{cell} is the current from a single cell. Besides, a constant two appears in the denominator of (12), since both charging and discharging current values are considered.

Based on the above-mentioned analyzes, Fig. **??**(b) schemes the battery EoL cycle number N_{EoL} and battery SoH degrading rate $\dot{SoH}(t)$ under different c-rates ($c_{rate} \in [0, 10]$). Specifically, the SoH degrading rate (red curve) increases with the growth of c-rate, and such tendency becomes dramatically under high c-rates (e.g. $c_{rate} \geq 8$). Besides, it can be observed that battery tends to undergo more EoL cycles at medium crates (e.g. $c_{rate} \in [2, 5]$) than at low c-rates. This is because the adopted battery degrading model also includes the calendar-life effects.

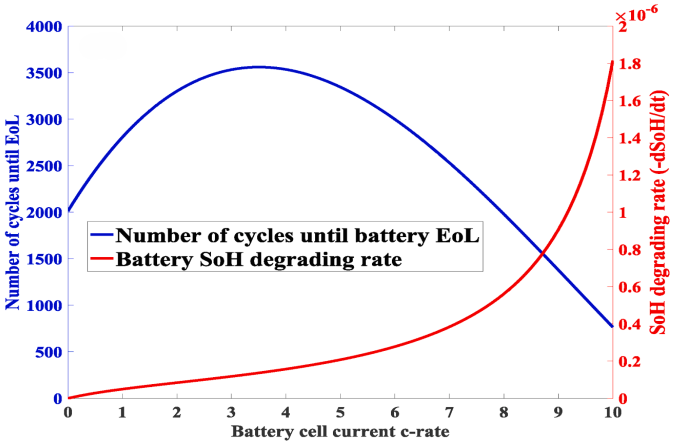

Figure 3. Battery health model: Blue curve is the relationship between c_{rate} and N_{EoL}. Red curve is the relationship between c_{rate} and battery SoH degrading rate $-\dot{SoH}(t)$

2.4. Electric machine model

Electric machine (EM) converts the input electrical power to mechanical power for vehicle propulsion, or to help recover a fraction of vehicle's kinetic energy. Based on the vehicle's power and torque requests from driving cycles, this paper adopts a Westinghouse 75-kW AC induction motor model from ADVISOR.

3. Cost optimization strategy via MPC

This section presents the development of the cost-minimization strategy via model predictive control (MPC), with its schematic diagram given in Fig. 4. First of all, a driving cycle is assigned, which contains information regarding the speed and acceleration that must be pursued throughout the driving test; in general, we would assume that at time k the speeds and accelerations that will occur throughout the established prediction horizon are known. This sequence enters a *Supervisor block* , the purpose of which is to predict the power demand along the entire horizon, knowing the speeds and accelerations that will be needed simulating the dynamics of the vehicle under examination. The predicted power sequence goes inside the blue box, named as *Decision-making level*: here the MPC, minimizing the vehicle's operating cost, calculates the control sequence to be applied along the time horizon in order to guarantee optimal energy management inside the car.

3.1. Formulation of MPC framework

In the predictive control framework, the length of control horizon is set the same as its prediction horizon (Hp), with the sampling period ΔT = 1s. Besides, the manipulated variable is selected as the increment of fuel cell power per step: $u(k) = \Delta P_{FC}(k) = \frac{P_{FC}(k)-P_{FC}(k-1)}{\Delta T}$, the state vector is formulated as: $x(k) = [SoC(k), P_{FC}(k-1), SoH(k)]$, and the DC bus power demand over the k-th horizon is deemed as the disturbances: $w(k) = [P_{dc}(k), P^*_{dc}(k+1), \ldots, P^*_{dc}(k+Hp-1)]$, wherein P^*_{dc} is obtained based on vehicle's dynamics, Eqs. (1) and (2).

3.1.1) Multi-objective cost function: To mitigate the vehicle's operating cost, a multi-objective performance index is used for optimization in this work, which incorporates the hydrogen consumption and the degradations of energy sources. In the k-th receding horizon, the designed MPC cost function can be expressed as:

$$J_k = C_{H_2,k} + C_{FC,k} + C_{BAT,k} + L_{SoC,k} \tag{13}$$

where $C_{H_2,k}$ is the hydrogen consumption cost, which can be calculated by:

$$C_{H_2,k} = p_{H_2} \cdot \frac{M_{H_2,k}}{1000} = p_{H_2} \cdot \sum_{p=0}^{p=H_p-1} \frac{P_{H_2}(P_{FC}(k+p))}{1000 \cdot LHV_{H_2}} \Delta T \tag{14}$$

where p_{H_2} is the hydrogen price per kilogram, $\frac{M_{H_2,k}}{1000}$ the hydrogen mass consumption in kilogram, and the quadratic fitted relationship between P_{FC} and P_{H_2} is given by Eq. (4). Additionally, the fuel cell degradation cost $C_{FC,k}$ is expressed as follows:

$$C_{FC,k} = C_{cycle,k} + C_{high,k} + C_{low,k} + C_{shift,k} \tag{15}$$

where $C_{cycle,k}$ is the degrading cost caused by fuel cell start-stop cycling, which can be calculated as:

$$C_{cycle,k} = \frac{\alpha_{on-off} \cdot N_{cycle,k}}{U_{EoL,FC}} \cdot p_{stack} \tag{16}$$

where $N_{cycle,k}$ is the number of fuel cell start-stop cycles over the k-th receding horizon, $U_{EoL,FC}$ (μV) is the voltage drop until the end-of-life (EoL) for a single fuel cell. Typically, ten percent of voltage drop of a fuel cell at the rated current density is deemed as the failure threshold. Moreover, p_{stack} is the price of the fuel cell stack.

In addition, fuel cell degradation costs owing to high and low loadings are given by:

$$C_{high,k} = \frac{\alpha_{high} \cdot \frac{T_{high,k}}{3600}}{U_{EoL,FC}} \cdot p_{stack} \tag{17}$$

$$C_{low,k} = \frac{\alpha_{low} \cdot \frac{T_{low,k}}{3600}}{U_{EoL,FC}} \cdot p_{stack} \tag{18}$$

where $\frac{T_{high,k}}{3600}$ and $\frac{T_{low,k}}{3600}$ are the duration (in hour) of fuel cell high and low loadings over the k-th horizon, respectively. Finally, fuel cell degradation cost induced by transient loadings is defined as:

$$C_{shift,k} = \frac{\alpha_{shift} \cdot \sum_{p=0}^{p=H_p-1} \frac{|\Delta P_{FC}(k+p)| \cdot \Delta T}{1000 \cdot N_{FC}}}{U_{EoL,FC}} \cdot p_{stack} \tag{19}$$

where N_{FC} = 300 is the number of cells in the stack. Furthermore, battery degradation cost ($C_{BAT,k}$) can be formulated as:

$$C_{BAT,k} = (SoH(k) - SoH(k+H_p)) \cdot p_{BAT} \tag{20}$$

where

$$SoH(k+1) = SoH(k) - \frac{\left|i_{cell}(k)\right| \cdot \Delta T}{2 \cdot N_{EoL}(c_{rate}) \cdot Q_{cell}} \tag{21}$$

and p_{BAT} is the price of battery pack. In this work, the parameters for cost calculation are taken from the referenced article [2]. In addition to the aforementioned cost terms, another term $L_{SoC,k}$ for penalizing battery over-charge or over-discharge is also integrated into the objective function of MPC, so as to maintain SoC around the initial value (SoC_{ini}) to the utmost extent.

$$L_{SoC,k} = w_{SoC} \cdot \sum_{q=0}^{q=H_p} (SoC(k+q) - SoC_{ini})^2 \tag{22}$$

where

$$SoC(k+1) = SoC(k) - \frac{\eta_{|BAT} \cdot I_{BAT}(k) \cdot \Delta T}{Q_{BAT}} \tag{23}$$

w_{SoC} is a constant positive weighting coefficient, which should be tuned via trials and errors.

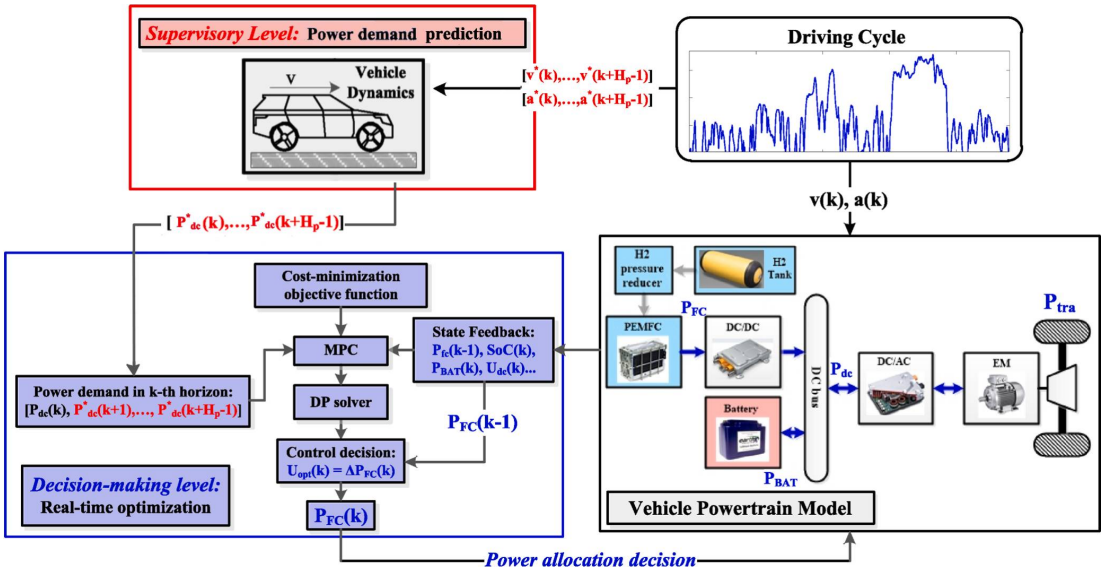

Figure 4. Predictive control framework of the proposed cost minimization strategy.

3.1.2) Constraints: To ensure the normal operation of powertrain components, several constraints should be enforced when making power-splitting decisions. Firstly, the constraints on fuel cell power and the changing rate of fuel cell power are denoted as:

$$P_{FC}^{min} \le P_{FC}(k+p) \le P_{FC}^{max}, p \in \{0, 1, ..., H_p - 1\} \quad (24)$$

$$\Delta P_{FC}^{min} \le \Delta P_{FC}(k+p) \le \Delta P_{FC}^{max}, p \in \{0, 1, ..., H_p - 1\} \quad (25)$$

where P_{FC}^{min} = 0W, P_{FC}^{max} = 30000W, $\Delta P_{FC}^{max} = -\Delta P_{FC}^{min}$ = 1000W/s.

In addition, battery current should be bounded by:

$$I_{BAT}^{min} \le I_{BAT}(k+p) \le I_{BAT}^{max}, p \in \{0, 1, ..., H_p - 1\} \quad (26)$$

In this work, we assumed that 97 ANR26650M1 cells (3.3 V/2.3 Ah) are connected in series to form a module, and ten such modules are aggregated in parallel to form the studied 7.4kWh (320 V/23 Ah) battery pack, with all integrated cells assumed to be in the identical electrochemical status. Thus, the current from each battery cell can be calculated by averaging the current from battery pack: $i_{cell} = I_{BAT}/10$. In this case, $I_{BAT}^{min} = 10 \times (-35)$A and $I_{BAT}^{max} = 10 \times (70)$A. Moreover, battery SoC and SoH should be subject to the following constraints:

$$SoC^{min} \le SoC(k+p) \le SoC^{max}, p \in \{0, 1, ..., H_p - 1\} \quad (27a)$$

$$SoC(k+1) = SoC(k) - \frac{\eta_{BAT} \cdot I_{BAT}(k) \Delta T}{Q_{BAT}} \quad (27b)$$

$$SoC(0) = SoC_{ini} \quad (27c)$$

$$SoH^{min} \le SoH(k+p) \le SoH^{max}, p \in \{0, 1, ..., H_p - 1\} \quad (28a)$$

$$SoH(k+1) = SoH(k) - \frac{|i_{cell}(k)| \Delta T}{2 \cdot N_{EoL}(c_{rate}) \cdot Q_{cell}} \quad (28b)$$

$$SoH(0) = SoH_{ini} \quad (28c)$$

where SoC^{min} = 0.58, SoC_{max} = 0.82 and SoC_{ini} = 0.7. SoH_{min} = 0, SoH_{max} = 1 and SoH_{ini} = 1.

3.2. Solving optimization problem via dynamic programming

To obtain the power-allocating decision over the k^{th} receding horizon, following finite-horizon optimization problem needs to be tackled:

$$\min_{\Delta P_{FC}(k+p) \in \pi_{FC}, p \in \{0,1,..,H_p-1\}} J_k = C_{H_2,k} + C_{FC,k} + C_{BAT,k} + L_{SoC,k}$$
$$\text{subject to} \quad \text{Eq. (24)-(28)} \quad (29)$$

where P_{FC} is the discrete feasible set of the manipulated variable ΔP_{FC}. Obviously, since some of the cost terms in J_k are not in the linear or quadratic form of ΔP_{FC}, problem Eq. (29) is thus a nonlinear optimization problem. Hence, dynamic programming (DP) is used to tackled such problem. Once the optimal control sequence $[\Delta P_{FC}^*(k), \ldots, \Delta P_{FC}^*(k+Hp-1)]$ is derived, only the first element $\Delta P_{FC}^*(k)$ is applied to the plant model, while the others are discarded. With the system states renewed at the next time step, the optimization is performed again to seek the next control action.

4. Results

In this section, the cost-optimization framework would be integrated with MPC and power demand-forecast result, so as to control the power flow between fuel cell and battery for different driving cycles. To evaluate the performance of the proposed EMS, firstly, a sensitivity analysis is conducted to explore the impacts on EMS performance with different weights (w_{SoC}) that penalize both battery over-charge and over-discharge. The performance of the proposed strategy is then compared to a rule-based strategy to reveal its advantages.

4.1. Cost function

To fairly compare the performance of different control strategies we introduce a function that quantifies the vehicle's total operating cost over a given driving cycle:

$$C_{total} = \sum_{k=0}^{k=T_{cycle}-1} C_{H_2}(k) + C_{FC}(k) + C_{BAT}(k) + C_{Elec}(k) \quad (30)$$

where T_{cycle} is the duration of the driving cycle, C_{H_2},C_{FC} and C_{BAT} are the previously given in 3.1.1. The last term C_{Elec} reflects the equivalent hydrogen consumption cost imposed by battery SoC variation, which is defined as:

$$C_{Elec}(k) = p_{H_2} \cdot \frac{M_{Elec}(k)}{1000} = \\ = p_{H_2} \cdot \frac{\Delta SoC(k) \cdot E_{BAT} \cdot 3600}{1000 \cdot \eta_{|FCS}(P_{FC}(k)) \cdot LHV_{H_2}} \quad (31)$$

4.2. Driving cycle

Two driving cycles were considered to evaluate the performance of the implemented control strategy. These cycles test the vehicle under different conditions, demonstrating the efficiency of the strategy in both scenarios.

The first one is ARTEMIS, which simulates an urban driving scenario characterized by periodic stretches of speed ranging between 0 and 60 km/h. In this cycle, the vehicle stops for brief moments, then accelerates to the maximum speed, maintains a constant speed for a few seconds, and then decelerates.

The second one is US_06_HWY, a typical high-speed driving cycle designed to simulate highway conditions, testing the vehicle starting from low speeds, maintaining an average speed of 120 km/h for most of the time, and then simulates a gradual stop.

4.3. Effect of Initial Guess for Optimizer

A properly configured standard Linear MPC optimization problem has a unique solution. However, Non Linear MPC optimization problems often allow multiple solutions (local minima), and finding the optimal solution can be difficult for the solver. In such cases, it is important to provide a good starting point near the global optimum. Since our problem is formulated as a Non Linear MPC, we had to find a way to supply our solver an initial guess for every simulation. After some trials, we decided to relate the initial guess for finding the optimal solution to the weight coefficient w_{SOC}. The best option we reached is to use as initial P_{FC} a percentage of (1-$\%_{BAT}$) where $\%_{BAT}$ is obtained as follows:

$$\%_{BAT} = \frac{11}{24} - \frac{1}{12} \cdot w_{SOC} \quad (32)$$

4.4. Effect of State-Of-Charge weighting factor

The SoC weighting factor w_{SOC} affects the SoC regulation performance. On this basis the EMS is evaluated under different w_{SOC} (1,4,10) candidates, for both ARTERIAL and US_06_HWY driving cycle. Fig. 5 below shows the results of the ARTERIAL driving cycle using different w_{SOC} values. As can be seen, the choice of this factor influences both the state variables of the problem and the resulting control input. Specifically, as w_{SOC} increases, the strategy tends to preserve the batteries by favoring a higher hydrogen consumption. For w_{SOC} = 10, the fuel cell demand is the highest, the SoC never drops below 0.7 (meaning the batteries never discharge significantly), and the SoH decreases more gradually. Finally are shown the results of the overall hydrogen consumption and the total costs parameterized with respect to w_{SoC} using the implemented control strategy. It can be observed that a lower w_{SoC} promotes lower hydrogen consumption, but results in a higher total cost for the vehicle's overall driving. Therefore, w_{SoC} = 10 proves to be the optimal choice for this factor in the simulation of the ARTERIAL driving cycle.

Next, an analogous analysis to the one previously conducted for the ARTERIAL driving cycle was performed for the US_06 driving cycle. The trend of the graphs shown in Fig 8 for different w_{SoC} values confirms what we have just observed for the ARTERIAL driving cycle, validating the previous evaluations. Notably, in this case, the choice of w_{SoC}=10 keeps the total costs significantly lower than the other choices. This is because, during the final deceleration, the controller performs a stop-start cycle, leading to a spike in total costs. This spike can be avoided by preserving the battery and increasing the demand on the fuel cell.

4.5. Performance comparison with Advisor Series Thermostat Control Strategy

The Series Thermostat Control Strategy implemented in Advisor is a rule-based strategy that determines at what torque and speed the engine should operate, to generate electric power via the generator, given the conditions of the motor, battery pack, and/or the engine/fuel converter itself. The rules are the following:

- The Fuel converter turns on if the SoC is below the low limit.
- The fuel converter remains on until the SoC reaches the high limit, if its previous state was on. After reaching the high limit, it turns off.
- The fuel converter operates at the most efficient speed and torque level.

The MPC-based and rule-based strategy are compared under US_06_HWY driving cycle, assuming w_{SoC}=10 for the MPC strategy. As seen in the Fig. 9, with w_{SoC} set to 10, the cost minimization strategy tends to consume more hydrogen than the rule-based strategy. In the rule-based approach, the engine operates at the optimal working point regardless of the SoC (in fact, when the SoC is above the maximum threshold, the engine is turned off), leading to lower hydrogen consumption. However, when comparing the total costs, the cost minimization strategy ensures a lower overall value.

When evaluating the effectiveness of the MPC, it should be noted that:

The total cost for the rule-based strategy, do not account for the term related to SoH, as it is not provided by ADVISOR. The MPC makes choices that also preserve the battery's SoH,

maintaining the vehicle's health throughout the driving cycle. Overall, the cost minimization strategy offers the following trade-off: it consumes slightly more hydrogen but ensures lower final costs and a better State-of-health for the battery pack.

APPENDIX

This section will briefly describe the organization of the project from a code writing point of view.

The work has been based on the utilization of three softwares: MATLAB, Simulink and ADVISOR.

The entire project is organized in a folder which contains the main Scripts of the project and also two more folders: one, namely "Functions", dedicated to the storing of the functions used by the main scripts and another, namely "Simulazioni", in which store the results data and graphics.

A. ADVISOR

ADVISOR has some default car models and a variety of internal components that can be freely adjusted from their .m files that can be found in ADVISOR installation folder. In particular, we needed to adapt Fuel Cells, ESS and the control logic to the ones adopted in the paper. To this end we developed some patch files that conveniently modify the internal resistance and tension values of each battery cell and the maximum power of the fuel cell system. Furthermore, the logic controller has been changed directly from the .xls Simulink model.

B. SIMULINK

Simulink car model has been changed to implement MPC controller and to move data between Simulink diagram and MATLAB Workspace. The main changes concern the "fuel cell <cs> config" and the "fuel cell config" block and can be inspected internally from the diagram.

C. MATLAB

The design of the nonlinear MPC, the model of the system, the definition of constraints, global variables and goal function have been realized in MATLAB scripts. The flow of the simulation runs as follows:

1) Firstly, the "config.m" script is called. This script allows to select the intended driving cycle to be simulated, tune the cost parameters and set the folder in which to save simulation results;
2) Afterwards, the "main.m" script is called, from which the MPC controller is defined and initialized;
3) Then, ADVISOR takes the control of the environment and starts vehicle simulation;
4) At the end of the simulation, the "endConfig.m" script is called which saves simulation data into the specified folder and runs some basilar plots to get an overall idea of the evolution of the main system variables.

REFERENCES

[1] "Advisor. advanced vehicle simulator." [Online]. Available: http://adv-vehicle-sim.sourceforge.net/

[2] Y. Zhou, A. Ravey, and M.-C. P'era, "Real-time cost-minimization power-allocating strategy via model predictive control for fuel cell hybrid electric vehicles," *Energy Conversion and Management*, vol. 229, p. 113721, 2021.

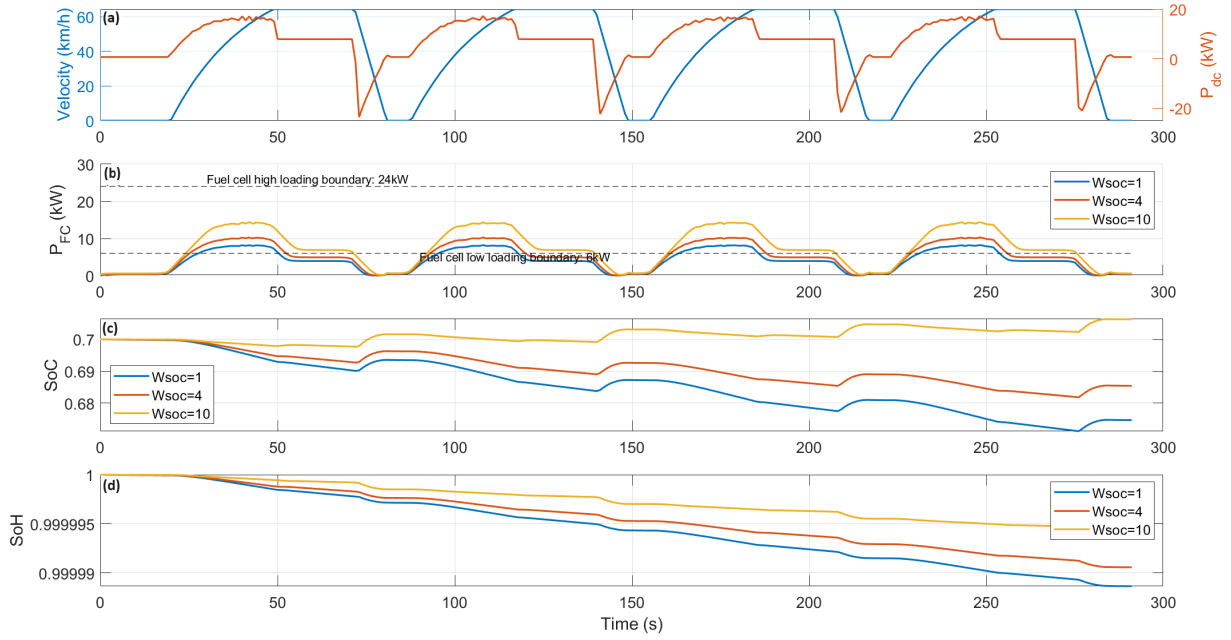

Figure 5. Impacts on EMS performance by w_{SoC}: (a) Speed and power demand profiles of ARTERIAL driving cycle; (b) fuel cell output power profiles under different w_{SoC}; (c) SoC evolution under different w_{SoC}; (d) SoH evolution under different w_{SoC}.

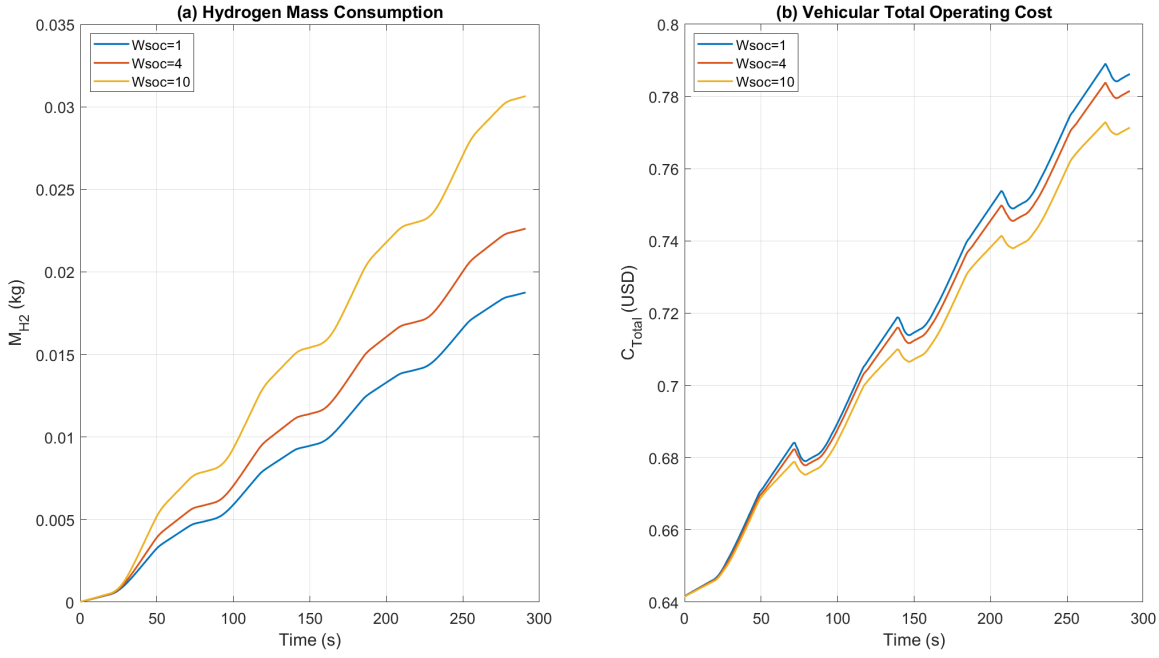

Figure 6. (a) Hydrogen mass consumption for different w_{SoC}; (b) Vehicular total operating cost for different w_{SoC}.

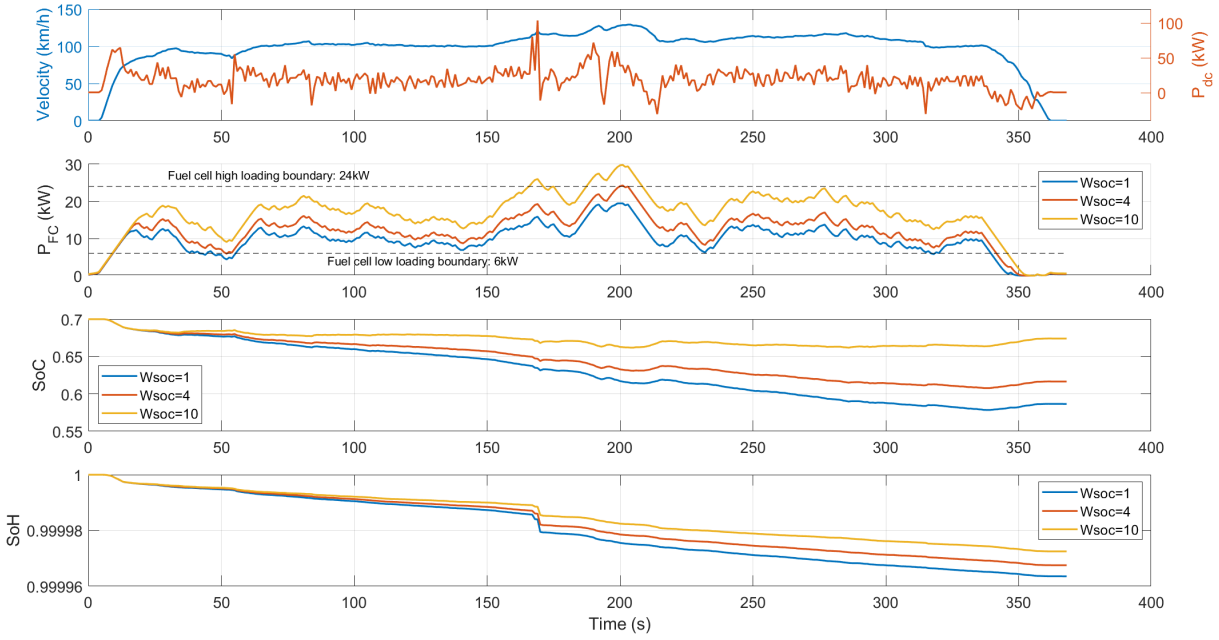

Figure 7. Impacts on EMS performance by w_{SoC}: (a) Speed and power demand profiles of US_06_HWY driving cycle; (b) Fuel Cell output power profiles under different w_{SoC}; (c) SoC evolution for different w_{SoC}; (d) SoH evolution for different w_{SoC}.

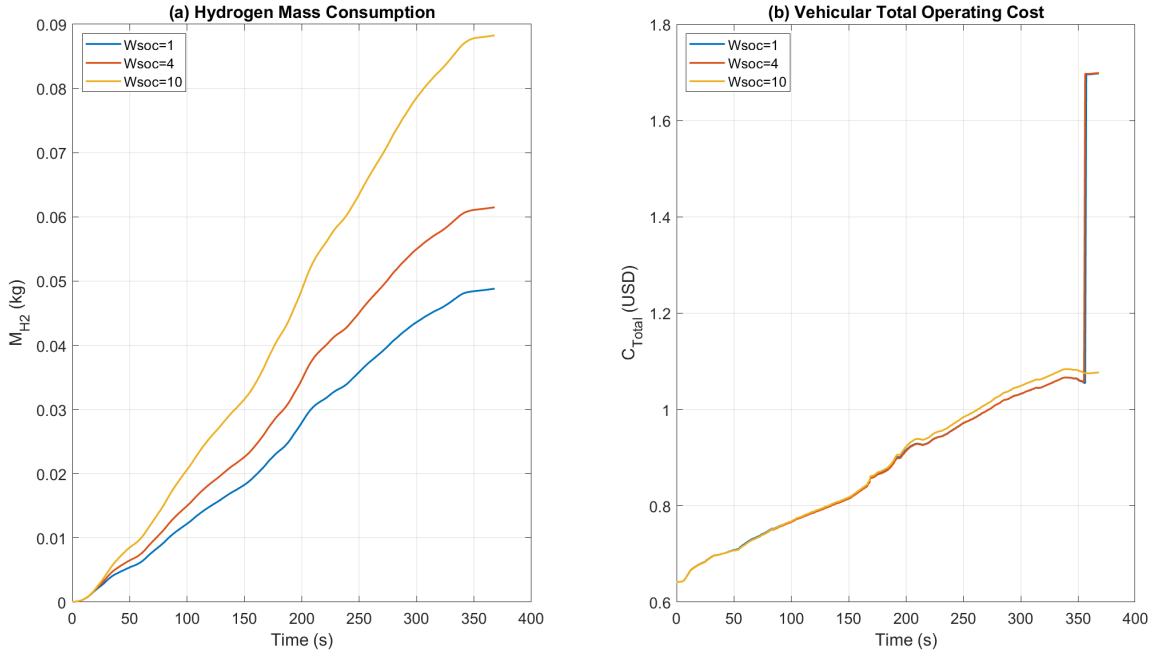

Figure 8. (a) Hydrogen mass consumption under different w_{SoC}; (b) Vehicular total operating cost for different w_{SoC}.

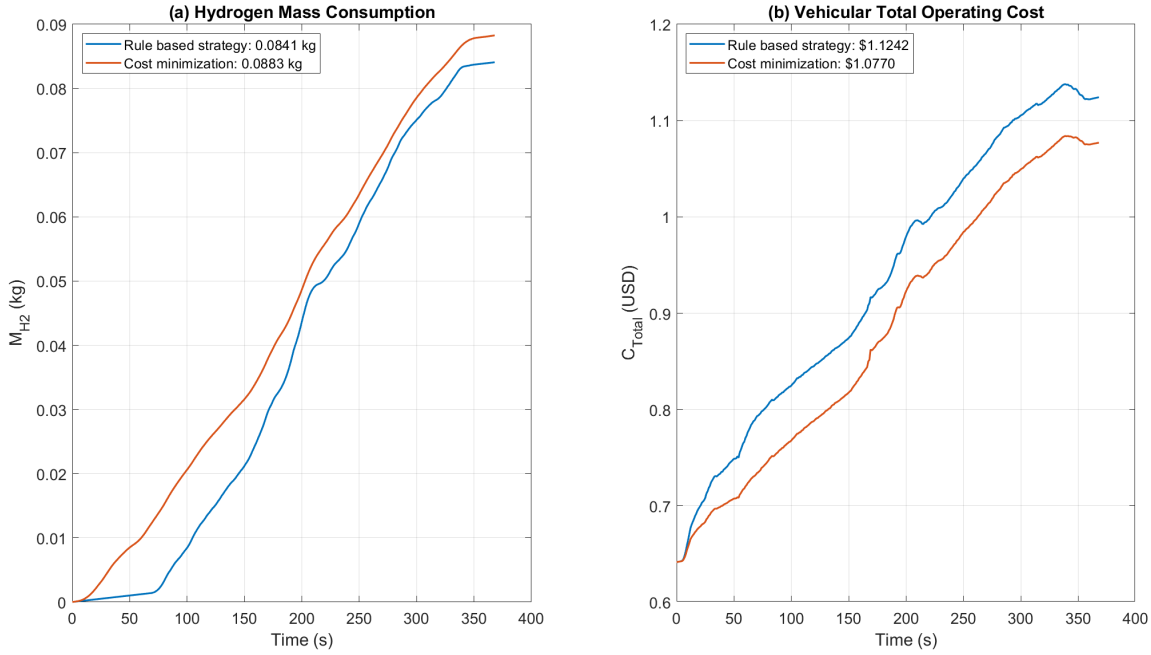

Figure 9. Rule based vs MPC based strategy: (a) Hydrogen mass consumption; (b) Veihicular Total Operating Cost;